Non-linear behaviour of nitric oxide reduction reactions over metal surfaces

1997 J. Phys.: Condens. Matter 9 1889

(http://iopscience.iop.org/0953-8984/9/9/006)

J. Phys.: Condens. Matter **9** (1997) 1889–1917. Printed in the UK PII: S0953-8984(97)75366-9

REVIEW ARTICLE

Non-linear behaviour of nitric oxide reduction reactions over metal surfaces

N M H Janssen, P D Cobden and B E Nieuwenhuys

Leiden Institute of Chemistry, Gorlaeus Laboratories, Leiden University, PO Box 9502, 2300 RA Leiden, The Netherlands†

Received 13 June 1996, in final form 6 December 1996

Abstract. Chemical reactions carried out under strongly non-equilibrium conditions can result in a variety of interesting effects such as oscillations, chemical waves, kinetic phase transitions, bistability, instabilities and chaos—all of these effects being mathematically due to the strong non-linearities in the kinetic rate equations describing these chemical processes. The present article reviews the various types of non-linear behaviour observed in several NO reduction reactions over Pt-group metals. A large part of this review deals with oscillations and spatiotemporal pattern formation in the NO–H_2 reaction over Rh surfaces: the reaction dynamics of this system has been realized on the microscopic, mesoscopic and macroscopic scales using field emission microscopy, photoemission electron microscopy and macroscopic rate measurements respectively. The various mechanisms of this and the other reactions reviewed in this article are also considered.

1. Introduction

The study of oscillating reactions has become a prominent research topic in the past 30 years or so. Pioneering work of Lotka in 1910 already showed that in an autocatalytic reaction the concentration of a reaction intermediate could approach a steady state through damped oscillations. In 1920 Lotka [1] showed that the concentrations of the intermediates may undergo sustained oscillations if there are two or more successive autocatalytic steps in the reaction.

One of the best known experimentally observed examples of oscillatory behaviour is provided by the Belousov–Zhabotinskii reaction, in which the overall reaction involves the oxidation of malonic acid by bromate in aqueous acid solution in the presence of a redox couple such as Ce^{III}/Ce^{IV}. The oscillations are usually observed by adding an indicator whose colour changes periodically as a result of repetitive fluctuations in the Ce^{III}/Ce^{IV} ratios. The mechanism involves a large number of steps and intermediates [2]. The first findings of Belousov were submitted for publication to various journals. The manuscripts were refused publication, since the results were considered to be artefacts due to experimental errors. Finally, one journal accepted a paper [3] and Belousov died not realizing that his work would have a great impact on chemistry and physics. Later, Zhabotinskii confirmed Belousov's results [4] and it was finally accepted that a chemical reaction taking place under constant reaction conditions can occur with more than one rate [5]. This type of metal-ion-catalysed bromination is now known under the name *Belousov–Zhabotinskii reactions*.

† Tel: (31) 71 5274545; fax: (31) 71 5274251.

0953-8984/97/091889+29$19.50

There is no doubt that also in the field of heterogeneous catalysis many researchers found in their work before 1970 variations in reaction rate with time of a type that we would call now oscillations. These results were, however, not published since fluctuations in rate were believed to be caused by noise or errors in the measuring devices. Since the first reports of rate oscillations in CO oxidation over metal catalysts, the study of oscillatory surface reactions has developed into a field of active research.

The purpose of this article is to review experimental work on the oscillatory behaviour of NO reduction over metal surfaces. The choice of examples presented in this paper is driven primarily by our own research interests and, therefore, does not represent the total body of relevant literature. Data on other than NO reduction reactions will be presented only to the extent that these results illuminate or complete the discussion. For recent general reviews on oscillatory catalytic reactions, we refer the reader to the references [6–12].

This review is organized in the following way. First a short summary is presented of the mechanisms of NO reduction over noble-metal surfaces. The specific differences in behaviour of Pt and Rh will be discussed. The following section presents an introduction to non-linear behaviour of surface reactions; mechanisms giving rise to oscillations are mentioned. The following sections deal with oscillations in rate and selectivity of NO reduction over Pt and Rh surfaces; spatial pattern formation observed by various techniques such as FEM (field emission microscopy), FIM (field-ion microscopy) and PEEM (photoemission electron microscopy) will be discussed. Finally, the last section will contain a general discussion, a brief summary and an outlook on future developments in our understanding of the intriguing field of oscillations in heterogeneous catalysis.

2. NO reduction by hydrogen, carbon monoxide and ammonia over noble metals of group VIII

This section reviews the current knowledge of the NO reduction reactions. The emphasis will be on the different behaviour of Pt and Rh surfaces in order to explain the specific differences found in the oscillatory behaviour of the NO reduction over the metals. The overall reactions are

$$2NO + 2H_2 \rightarrow N_2 + 2H_2O \tag{1a}$$

$$2NO + 5H_2 \rightarrow 2NH_3 + 2H_2O \tag{1b}$$

$$2NO + H_2 \rightarrow N_2O + H_2O \tag{1c}$$

$$2NO + 2CO \rightarrow N_2 + 2CO_2 \tag{2a}$$

$$2NO + CO \rightarrow N_2O + CO_2 \tag{2b}$$

$$6NO + 4NH_3 \rightarrow 5N_2 + 6H_2O. \tag{3}$$

The recent interest in reactions (1), (2) and (3) has been greatly stimulated by the relevance of these reactions in connection with automotive pollution control and NO_x removal from tail gases of stationary sources such as electricity plants [13]. In 1983 increasing stringency of legislative standards for automobile emission in the USA necessitated the introduction of the so-called three-way catalyst which is capable of controlling CO, hc and NO_x emission simultaneously using a single catalyst. This catalyst is based on Pt and Rh or Pd. The nitrogen oxides are converted into dinitrogen via reduction by hydrogen (process (1*a*)) and CO (process (2*a*)). Unfortunately, dinitrogen is just one of a variety of reaction products that can be formed in the catalytic converters used in

automobiles, due to the presence of various gases in the exhaust gas. One of the undesirable reaction products is NH_3, which is formed especially under reducing conditions via process (1*b*). NO removal from the gases of stationary sources such as electricity plants and nitric acid plants is more complicated because the reducing agent reacts more easily with the excess oxygen than with NO_x. The only reducing agent known that can selectively reduce NO_x in the presence of O_2 is ammonia via process (3). Again the Pt group metals are able to promote this selective reduction process. Pt is already a very active catalyst at low temperature. Complete conversion of NO_x can be obtained at 180 °C. However, above 200 °C the conversion decreases with increasing temperature, ultimately giving apparently negative conversion. The obvious explanation is NH_3 oxidation for which reaction Pt is an excellent catalyst; V, W and Ti oxides or their combinations are less active than Pt and, therefore, preferred for the selective reduction.

The first systematic studies of NO–CO and NO–H_2 reactions on supported noble metals were reported by Kobylinski and Taylor [14]. They found that the activity for the first reaction increases in the order Pt < Pd < Rh < Ru and for the second reaction in the order Ru < Rh < Pt < Pd. The first reaction is slower than the second; only for Ru was the order reversed. Ru is an excellent catalyst for the NO reduction with a minimum of NH_3 production. However, Ru forms volatile oxides under operating conditions, resulting in an unacceptable catalyst loss. The most efficient catalyst appears to be Rh [15].

Lambert and Comrie [16] studied the CO–NO reaction on Pt(111) and (110) surfaces and concluded that the reaction proceeds by a Langmuir–Hinshelwood mechanism between O and molecular CO.

Siera *et al* [17] studied the CO–NO reaction over a number of Pt–Rh alloy surfaces and compared the results with those found for the CO–O_2 reaction. At low temperatures (<500 K) the reaction rate increases in the order Pt–Rh(111) < (100) < (410) < (210). This is the same order as was observed for the CO–O_2 reaction and it corresponds to the order in heat of adsorption of CO. NO dissociation decreases in the order (410) ∼ (210) > (100) > (111). For both reactions the rate at low temperatures is controlled by CO desorption and not by NO dissociation.

Similar effects were found for the NO reduction by hydrogen over Rh single-crystal surfaces [18]. The initiation process is NO desorption. Surface structural effects are related to differences in the heat of adsorption of NO. Only at low NO coverages do the intrinsic differences in NO dissociation activity determine the surface structural effects.

Hirano *et al* [19, 20] studied in detail the NO–H_2 reactions on a number of pure Pt, pure Rh and Pt–Rh alloy surfaces. In particular, the mechanisms of the various processes resulting in the production of N_2, N_2O and NH_3 were investigated. For this purpose the authors studied the various reactions both in the 10^{-7} mbar range with access to surface analytical techniques and in the higher-pressure range. Isotopically labelled molecules were used in order to gather information concerning the mechanisms of the formation reactions of the N-containing products.

The main conclusions emerging from these studies are as follows.

(A) All three N-containing reaction products, N_2, NH_3 and N_2O, are formed via dissociation of NO:

$$NO_{ads} \rightarrow N_{ads} + O_{ads}. \tag{4}$$

(B) N_2 is formed by combination of two N adatoms over the whole temperature range (350–1300 K) studied:

$$2N_{ads} \rightarrow N_2. \tag{5}$$

(C) Below 600 K N_2 may also be formed via

$$NO_{ads} + N_{ads} \rightarrow N_2 + O_{ads}. \tag{6}$$

At higher temperatures the dominant mechanism is step (5).

(D) N_2O is formed via

$$NO_{ads} + N_{ads} \rightarrow N_2O \tag{7}$$

whose contribution decreases with increasing temperature and decreasing NO pressure, because of the lower NO coverage.

(E) NH_3 is formed via dissociation of NO and subsequent hydrogenation:

$$N_{ads} + 3H \rightarrow NH_3 \tag{8}$$

via a NH_{ads} intermediate.

(F) The availability of a vacant site near the NO_{ads} and N_{ads} may play a central role in the selectivity towards N_2O and N_2. A situation such as the one sketched as (ii) below, where □ denotes a vacant site on the surface, may result in N_2 formation, whereas situation (i) will result in N_2O formation:

O O O O
N N N N (i) □ N N (ii).

(G) Both the activity and the selectivity depend strongly on the surface structure and composition, as is shown in figure 1. In the low-temperature range ($T \sim 520$ K) the activity of the (100) surfaces decreases in the order Pt(100) > Pt–Rh(100) > Rh(100). The selectivity towards N_2 decreases in the order Rh(100) > Pt–Rh(100) > Pt(100). It is well established that a number of vacant metal sites are required before NO dissociation can occur. It was estimated that 4 to 5 vacancies are needed to dissociate NO on Rh(111) [21]. If the surface is largely covered with molecularly adsorbed NO or with N adatoms the reaction is inhibited by blocking of active sites. The conversion of NO at temperatures below 600 K is low for the Rh(100) surface due to the presence of strongly bound N atoms. The high selectivity of this surface is also caused by the high concentration of N adatoms. On Pt(100) the Pt–N bond strength is much weaker resulting in a much lower concentration of N adatoms at 520 K. Free Pt sites remain available and, consequently, the reaction rate is fast with, however, a much lower selectivity towards N_2. The Pt–Rh(100) alloy surface shows a behaviour intermediate of those of pure Pt and Rh(100). The NO–H_2 reaction on Pt(100) has been studied recently by Zemlyanov *et al* [22] using HREELS. The results confirm the appearance of an imide (NH_{ads}) species.

Belton and co-workers have studied in detail the NO–CO reaction over Rh(111) with the purpose of achieving an understanding of the elementary steps [23]. In addition, these authors investigated N_2 desorption from coadsorbed isotopically labelled NO and N [24] and desorption of N_2 from atomic N [25] on the same surface. The authors concluded that the only route resulting in N_2 formation is via N combination. The repulsive interactions between adsorbed nitrogen atoms and between coadsorbed N and O can result in enhanced N_2 formation at relatively low temperatures. It was suggested that the competition between N and O atoms for the same threefold hollow sites may cause a phase transition at higher coverages with a destabilization effect on adsorbed N leading to enhanced desorption of nitrogen [21].

The NO–NH_3 reaction over Pt and Rh surfaces has not been studied in the same detail as the NO–H_2 and NO–CO reactions. The reaction products are N_2 and H_2O. N_2O formation has also been observed under certain conditions. Most probably, the mechanisms of N_2,

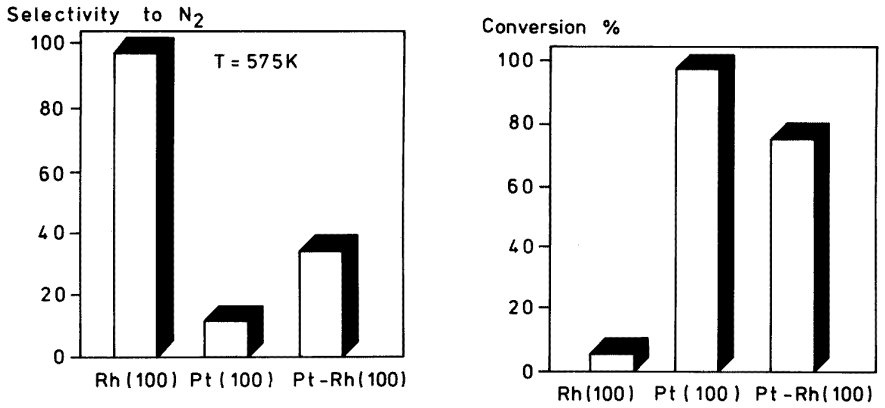

(a) (b)

Figure 1. NO conversion after three minutes of reaction time at 520 K (a), and selectivity towards N_2 determined at a total conversion of 100% (b) (adapted from reference [20]).

H_2O and N_2O formation resemble those discussed for the NO–H_2 reaction, with NH_3 being the source of hydrogen.

In conclusion, the surface science studies show that NO dissociation is a crucial step. Under steady-state conditions, the reaction is often inhibited by the presence of adsorbed CO or NO molecules. The data suggest a Langmuir–Hinshelwood mechanism between the O formed from NO dissociation and adsorbed CO or H.

3. Introduction of oscillatory behaviour of surface reactions

In this section a brief overview is presented of models proposed to describe the oscillatory behaviour of surface reactions. In addition, the concepts of spatial inhomogeneity and synchronization are introduced.

Why may a heterogeneous catalytic reaction exhibit oscillatory behaviour under certain conditions? It is realized now that there is no universal mechanism. For the sake of convenience, models for oscillations in surface reactions will be divided into two main categories: (I) non-isothermal models; and (II) isothermal models.

(I) *The non-isothermal model.* This model is one of the major mechanisms for oscillations of exothermic reactions over supported metal catalysts in the higher-pressure range. The heat released by the reaction cannot be transported sufficiently via the non-conducting support. The exothermic reaction starts, for example triggered by a surface defect or impurity. The energy released causes the metal particle to be heated resulting in an increase of the reaction rate. More heat is produced and, at a certain stage, the local temperature becomes too high for adsorption of the reactants. The reaction rate drops resulting in a decrease in temperature and the cycle starts again. Nice examples of non-uniform temperature distribution on supported metal catalysts during oxidation reactions have been shown by the group of Wolf [26]. Thermokinetic waves over the surface have been imaged by IR emission techniques [27, 28].

(II) *The isothermal model.* This general model can be subdivided into a number of classes which have in common a periodic transition between two surface states with different activities.

(IIa) Transitions between two states differing in *chemical composition*. Sales, Turner and Maple [29] associated the oscillations found for CO oxidation over supported noble metal catalysts with a slow and reversible modification of the catalyst composition: slow oxidation and reduction, inducing transitions between the two branches. As the activities of the oxidized and the reduced surface for CO_2 production are very different, oscillatory behaviour is observed. In a related model the less active surface contains carbon deposited on the surface [30]. The periods of this kind of oscillation are typically relatively long, usually between 5 and 100 minutes. Oscillations in the rate of the CO–NO over a Pt-ceria catalyst supported on γ-Al_2O_3 belong to this class [31].

(IIb) Adsorbate-driven transitions between two *surface structures* with different activities. The first reports of oscillations in the reaction rate for low-pressure reactions were for NO + CO over a Pt ribbon [32] and a Pt(100) surface [33]. Adloch *et al* [32] proposed that surface structure changes are responsible for the oscillatory behaviour. The first systematic and extensive studies for this reaction were performed by the groups of Ertl [34] and Schmidt [35]. The reaction studied in most detail was that of CO–O_2 over Pt(100) [7]. The clean Pt(100) surface reconstructs, i.e. the atomic arrangement in the topmost layer is not that of the corresponding bulk plane. However, the reconstruction is lifted by adsorption of CO and NO when the coverage exceeds a certain critical coverage. The driving force is the higher heat of adsorption of CO on the non-reconstructed surface which overcompensates the energy required for altering the surface structure. The sticking probability of oxygen is negligibly small on the reconstructed surface while it is much higher on the non-reconstructed surface. Ertl proposed the following model for the oscillations. The surface structure changes to the non-reconstructed surface due to CO adsorption. Oxygen can then be adsorbed due to the relatively high sticking probability on this surface. The adsorbed O reacts with adsorbed CO molecules to yield CO_2 that is immediately released into the gas phase. As a result more sites are created for oxygen adsorption and the reaction rate increases. The CO coverage decreases because of its rapid reaction with O. At the critical CO coverage the surface structure transforms back into the reconstructed phase. Oxygen ceases to be adsorbed and, hence, the reaction rate decreases. The CO coverage will then increase and beyond the critical coverage the surface structure transforms again to the non-reconstructed phase. This transformation completes the cycle of the oscillation.

(IIc) Transitions between two surface states with different concentrations of adsorbates. The *vacancy model* involves transitions between almost adsorbate-free and adsorbate-covered surfaces, the reaction is inhibited on the latter. This mechanism was proposed for, among others, the NO–CO [7] and NO–H_2 reactions over Pt(100) [36–38]. The essential steps are as follows. Dissociation of NO required for the reaction is inhibited by a high concentration of NO/CO. Vacancies are created, for example by some desorption of NO/CO. NO can then dissociate resulting in the initiation of the relevant reactions: N_2 formation by reaction (5) and H_2O (or CO_2) formation by reaction of H (or CO) with O. As a result more vacancies are created and the reaction rate increases in an autocatalytic way. A possible feedback mechanism may be inhibition of NO dissociation by build-up of O [37] which is more slowly removed by H(CO) than N by reaction (5). During the removal of O, NO is built up on the surface and the cycle starts again. No structural transition is required in this model. Also, a model proposed by Cutlip *et al* [39] for CO oxidation involving reaction only at the perimeter of CO and O islands belongs to class IIc. In addition, a model involving reversible formation and depletion of *subsurface O* which can also account for periodic modulations of the catalytic activity [40], is classified in category IIc. However, it should be noted that the subdivision of II into IIa, IIb and IIc is rather arbitrary.

Oscillations in the rates of catalytic reactions are usually monitored by following the concentrations of reactants and reaction products using *gas-phase analysis* by MS or GC or by following the processes *on the surface* by work-function measurements. However, non-linearity of a catalytic reaction is not only manifested by macroscopic rate oscillations but also by *spatiotemporal pattern formation* on the surface [9, 11, 12, 41]. In particular, the elegant studies of Ertl *et al* have provided a wealth of novel information concerning non-linear phenomena on surfaces [7, 12, 41]. The occurrence of thermokinetic waves caused by finite temperature differences for reactions at higher pressures have been mentioned already. At lower pressures spatiotemporal patterns have been observed for a number of reactions on various surfaces by means of the techniques of photoemission electron microscopy [9, 12, 41] (PEEM, resolution about 200 nm) and, more recently, by low-energy electron microscopy [42] (LEEM, resolution 10 nm) and mirror electron microscopy [43] (MEM, resolution 10 nm). Very recently, two optical techniques, namely ellipsometry for surface imaging and reflection anisotropy microscopy, have been applied to image pattern formation in surface reactions [44]. The advantage of these optical techniques is that they can be used both at low and atmospheric pressures.

Target patterns and rotating spiral waves are typical of chemical waves, i.e. concentration gradients travelling over the surface by diffusional coupling. Also Turing waves, i.e. stationary concentration patterns and chemical turbulence, the equivalent of chaos in pattern formation, have been found in surface reactions.

In the past four years the techniques of FEM and FIM have been used to investigate pattern formation on the (almost) atomic level [44, 45]. Several examples will be presented in this paper.

Synchronization between various parts of the surface is needed for the occurrence of macroscopic rate oscillations. Due to the spatial non-uniformities the contributions of the various local oscillators would otherwise average out to a stationary reaction rate. Usually three different mechanisms are considered for synchronization.

(A) *Heat transfer*. This is the dominant synchronization mode for non-isothermal oscillations at higher pressures (>1 mbar).

(B) *Gas-phase coupling*. Variations of local partial pressures due to local oscillations in reaction rate are rapidly transmitted to other parts of the system. The role of gas-phase coupling as a major mode of coupling for oscillations in surface reactions in the 10^{-5} mbar range was demonstrated by Ehsasi *et al* [46] for CO–O_2 on Pd(110). Two different Pd(110) crystals were used, both mounted in the same uhv chamber/reactor, but the crystals were not connected to each other. The oscillations were followed by work-function measurements. Synchronization of the macroscopic rate oscillations on the two surfaces was observed, which could be achieved only by gas-phase communication.

(C) *Coupling by surface diffusion of a mobile adsorbate*. FEM experiments for NO–H_2 over Rh using two single-crystalline tips separated by a grain boundary demonstrated the relevance of this communication mechanism for oscillations of rates of reactions on small crystals in the 10^{-6} mbar range [47].

4. Catalytic reduction of NO over Pt; oscillations in the rate and selectivity

This section summarizes data concerning oscillations in the rate and selectivity for the three NO reduction reactions, (1), (2) and (3), over Pt surfaces. The reactions have also been studied by FEM and FIM; these results will be discussed in a separate section together with FEM and FIM observations for these reactions on other metals.

For all of the NO reduction reactions, rate oscillations have only been observed on Pt(100) and polycrystalline Pt surfaces. The reactions have also been studied on Pt(111) and (110), but oscillations were not found. In fact, the reaction rates over these surfaces are much lower than over Pt(100) [48] as should be expected on the basis of the activities of these Pt surfaces in NO dissociation [49]. Studies of the NO–CO reaction on a cylindrically shaped Pt single crystal are consistent with these observations: oscillatory behaviour was only observed on surfaces from (100) to (310) which are quite active in NO dissociation [50]. Measurements for the NO–H_2 reaction over Pt field emitters are also consistent with these observations [51].

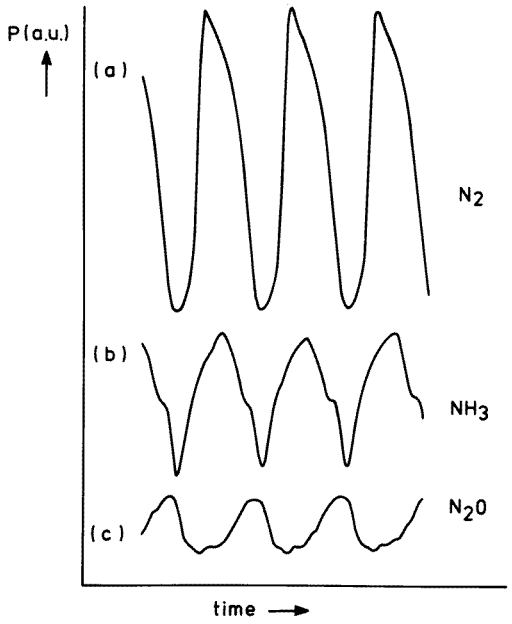

Figure 2. Variations of the N_2, NH_3 and N_2O partial pressures during the NO + H_2 reaction over Pt(100) as a function of time. $T = 460$ K, p(NO) and $p(H_2) = 3 \times 10^{-6}$ mbar (from reference [37]).

4.1. NO–CO

Schwartz and Schmidt [35] observed rate oscillations for the NO–CO reaction over Pt(100) for $p(\mathrm{NO})/p(\mathrm{CO})$ between 2 and 1, total pressures from 1×10^{-7} to 5×10^{-6} Torr and temperatures between 410 and 490 K. Oscillation periods were of the order of 1 minute. The period decreases and the temperature range for finding oscillations also decreases as the total pressure decreases. The authors associated the oscillations with the $(1 \times 1) \leftrightarrow$ hex surface phase transition of Pt(100). It was suggested that oscillations on polycrystalline or supported Pt are associated with oscillations on Pt(100) patches [35]. Veser and Imbihl [52] found two separate temperature regimes, depending on the NO and CO partial pressures, for the existence of non-linear behaviour for the reaction on Pt(100). In the low-temperature range, around 400 K, non-linear behaviour was observed by PEEM, but synchronization to macroscopic rate oscillations could only be transiently achieved by small temperature

jumps. The surface structure remains in the (1×1) phase. In the higher-temperature range (470–490 K) sustained oscillations were observed. The structure is largely in the hex phase and the oscillations are coupled to periodic structural changes via the $(1 \times 1) \leftrightarrow$ hex phase transition. Spatiotemporal waves are not found in the temperature regime where sustained oscillations are found, or, in other words, the oscillations proceed in a spatially uniform manner. The Feigenbaum route to chaos (see the section dealing with NO–H_2) has been observed.

Kinetic modelling has been performed by Fink *et al* [53] using the method of coupled differential equations which describe the following sequence of steps:

$$CO + \square \leftrightharpoons CO_{ads} \tag{9}$$

$$NO + \square \leftrightharpoons NO_{ads} \tag{10}$$

$$NO_{ads} + \square \rightarrow N_{ads} + O_{ads} \tag{11}$$

$$CO_{ads} + O_{ads} \rightarrow CO_2 + 2\square. \tag{12}$$

The autocatalysis in the creation of vacancies $\square$ and, hence, in the dissociation of NO, is the driving force for the oscillatory behaviour in the low-temperature regime. For the high-temperature regime the adsorbate-driven $(1 \times 1) \leftrightarrow$ hex phase transition was incorporated in the modelling.

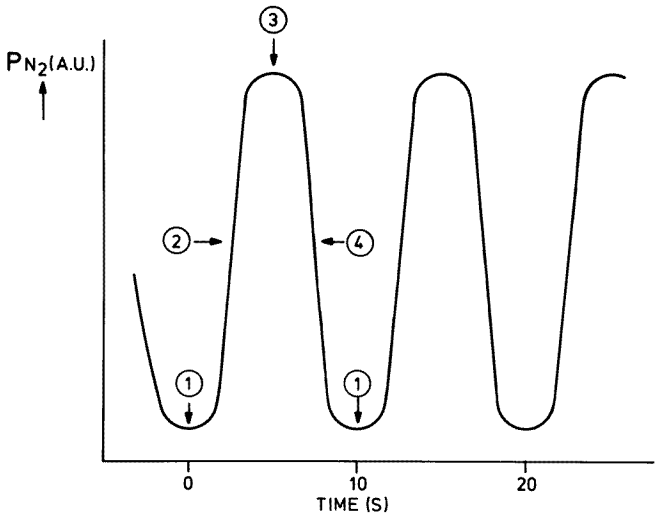

Figure 3. A schematic representation of an oscillation in the pressure of nitrogen versus time.

Recently, King *et al* [54] found that the (1×1) CO island growth rate is strongly non-linear in the concentration of CO on the hex phase: four CO molecules on the hex phase are involved in a concerted conversion of a hex-phase patch to (1×1) during the nucleation and growth of the (1×1) islands. To model the NO–CO reaction, Hopkinson and King [55] incorporated this new information in the calculations. For NO a similar non-linear (1×1) NO island growth rate was assumed as was found experimentally for CO. The authors concluded that their modelling reproduces the major observations of non-linear behaviour for the NO–CO reaction. Again, the driving force for the oscillatory behaviour in the low-temperature regime is the autocatalysis in the NO dissociation. In the higher-

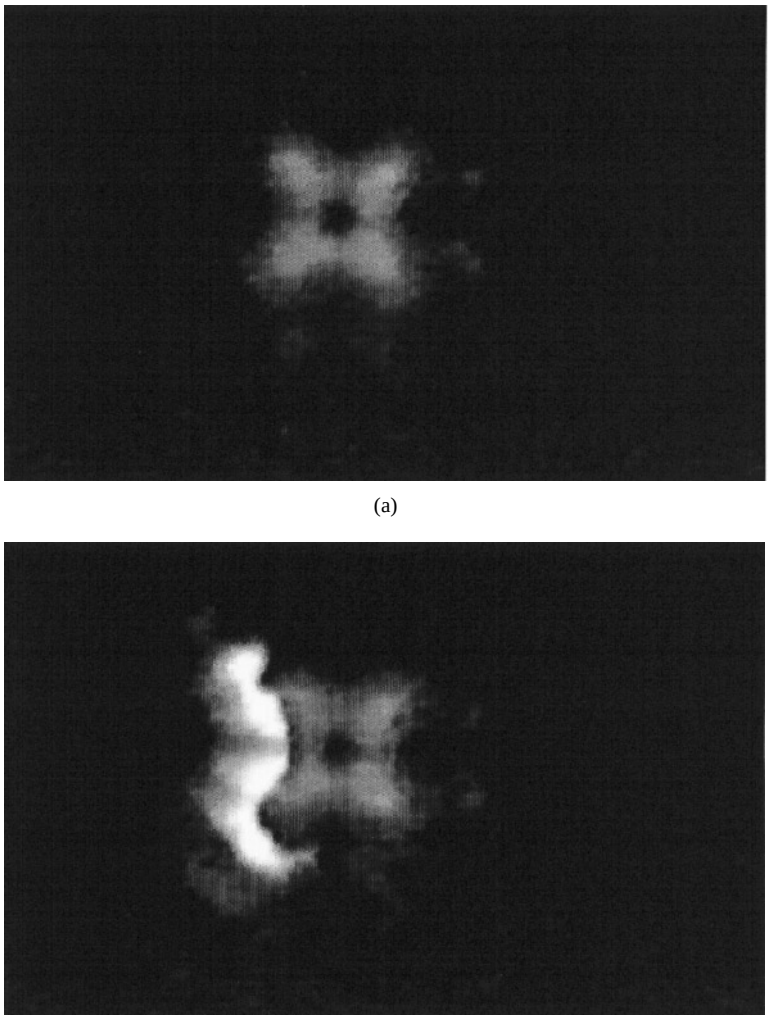

(a)

(b)

Figure 4. FEM images observed for the NO–H_2 reaction over a Rh field emitter at 460 K, 2×10^{-7} mbar NO and 1.3×10^{-6} mbar H_2. The images were recorded at (a) 0 s, (b) 3 s, (c) 12 s and (d) 17 s.

temperature regime the oscillations are not controlled by NO dissociation; the non-linear (1×1) growth rate plays a critical role.

4.2. NO–H_2 and NO–NH_3

The dynamic behaviours of these reactions over Pt(100) show many similarities. Macroscopic rate oscillations have been reported by Cobden *et al* [37], Siera *et al* [36], Slinko *et al* [38], and van Tol *et al* [56], in similar ranges of temperature and total pressure for both reactions. Sustained oscillations in rate have been observed from 430 to 500 K for NO/H_2 ratios varying from 2 to less than 0.1. Periods vary from less than 1 s at 500 K to more than 5 min in the low-temperature range. Figure 2 shows that also the *selectivity* to

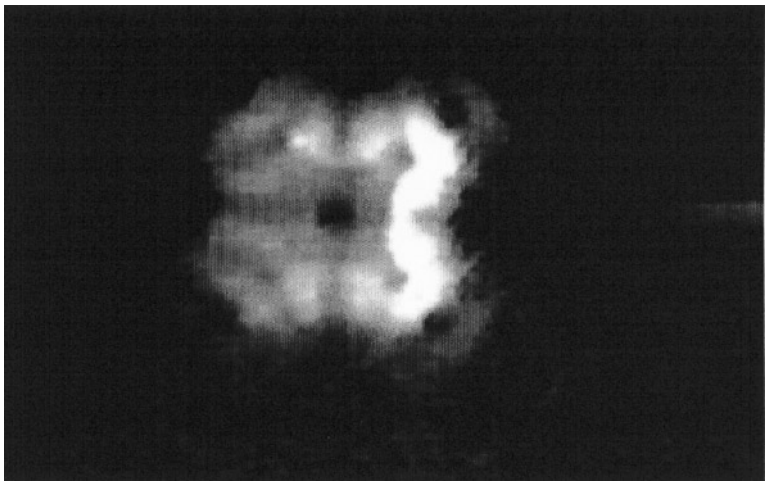

(c)

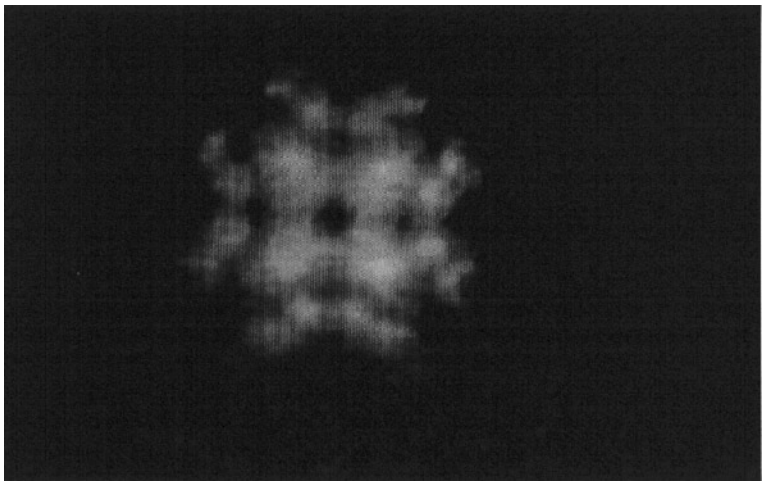

(d)

Figure 4. (Continued)

the products N_2, NH_3 and N_2O oscillates: the rates of N_2, NH_3 and H_2O oscillate in phase and in antiphase with N_2O. For NO–NH_3 the product pressures of N_2 and H_2O are in phase with each other but out of phase with the pressures of NH_3, NO and N_2O.

The Feigenbaum route to chaos was observed for both reactions: a series of period doublings by small changes in the reactants ratio, leading, finally, to a state of deterministic chaos or aperiodic behaviour. Cobden *et al* [37] and van Tol *et al* [56] described the oscillations for both reactions in terms of the vacancy model. The authors suggested that the $(1 \times 1) \leftrightarrow$ hex phase transition is not necessary for the oscillations. A schematic representation of the model is shown in figure 3.

At stage 1 the surface is covered with NO, only a few vacancies are present and the rate of N_2 production is low while the rate of N_2O formation is relatively high. Vacancies are created; the reaction rate to N_2 increases in an autocatalytic way as has been discussed before (stage 2). At stage 3 the N_2 production reaches its maximum value; the number

of vacancies is high. The reaction rate drops because the rate of NO adsorption becomes smaller than the reaction rate. NO is adsorbed on the relatively empty surface (stage 4). NO dissociation is inhibited by the presence of O which is removed relatively slowly by hydrogen.

The NO–H_2 and NO–NH_3 reactions were modelled in a similar way to that for NO–CO on Pt(100). The authors [57] suggested on the basis of PEEM observations for the NO–NH_3 [58] reaction that the $(1 \times 1) \leftrightarrow$ hex phase transition occurs during the oscillation. The most recent computer simulation of the oscillations for NO–H_2 over Pt(100) has been presented by Gruyters *et al* [59] using the strongly non-linear power law observed for (1×1) island growth from the hex phase [54]. The authors concluded that the driving force for the oscillations is a combination of the hex phase $\leftrightarrow$ (1×1) phase transition, the non-linearity in the (1×1) island growth and the low reactivity of the hex phase. An autocatalytic reaction enables a fast switch from the low- to the high-rate branch.

5. Spatiotemporal processes imaged on the atomic scale

Experimental techniques such as PEEM only allow spatial resolution on the mesoscopic scale (>1 μm). The introduction of FEM and FIM for following the progress of oscillatory processes increased the spatial resolution to the microscopic scale ($\sim$20 Å). This means that the total field of view resolved by these techniques is equivalent to the spatial resolution of a technique such as PEEM. The first FEM study to take advantage of this resolution in the analysis of an oscillatory process was the reduction of NO with H_2 over a Rh field emitter [60]. This was in fact the first report of such behaviour under high-vacuum conditions for this reaction over Rh. The first FIM study into oscillatory behaviour was the catalytic oxidation of CO over a Pt field emitter [45], a reaction which had already been extensively studied over Pt single-crystal surfaces (see for example [7]).

These techniques do however bring other complications with them. The sample is in the form of a metal tip of small radius (typically $\sim$1000 Å), a geometry which is needed to create the high field strengths (typically $\sim$0.1 V Å^{-1}–1 V Å^{-1}) required for these techniques. The role of such high electric fields, especially in FIM, has been brought into question. For example, the H_2–H_2O reaction over a Pt field emitter, as studied with FIM, showed oscillatory behaviour which could be associated with field effects [61]. However, the effect of the field in FEM experiments, which uses a lower field strength than FIM, has not been shown to be of anything but negligible importance. The sample also contains many different crystallographic orientations which can also interact with each other [62]. This was clear form the very first FEM study where most of the planes taking part in the oscillation do so as a result of a nearby plane undergoing changes [60].

5.1. NO reduction with H_2 over Rh field emitters

After the introduction of a flow of NO and H_2, a Rh tip was heated slowly in the applied field. At 530 K, an increase in the emission began on the (321), (533) surfaces. This increase in emission spreads in the direction of the (311) and (320) surfaces to such an extent that almost all of the planes present on the tip have undergone an increase in emission current [60]. The (100) plane and its surroundings did however remain dark. Such a sharp moving front has been reported before the reaction of O_{ads} and NO_{ads} layers with hydrogen [51, 63]. The increase in emission was initially interpreted as a change from a NO_{ads} to a N_{ads} adlayer [51], but it could equally be interpreted as the removal of work function increasing O_{ads} from the surface.

On subsequent cooling, sustained oscillations were observed at 460 K, as illustrated in figure 4. The oscillations take the form of a wave, which moves around the surface and is associated with an increase in the emission current [60]. The increase in emission begins around the (533) and (321) planes and essentially moves around the tip parallel to the step edges. This wave is also seen to move more quickly along the surfaces with (111) terraces and (100) steps, such as (533), than along the surfaces with (110) terraces and (100) steps, such as (320). After 14 s, the wave has spread across the whole surface, with the exception of the (100), (210) and areas around the (211) which do not appear to take part in the oscillations. The emission intensity starts to decrease beginning around the smoother planes around the (100) surfaces, and between the (111) and (100) planes [60]. The oscillations were sustained for many hours, and were not influenced noticeably by changes in the applied field. Under the same conditions, but at the lower temperature of 430 K, the four quadrants of the [100]-oriented tip are seen to act independently of each other [60, 64]. The wave does not spread over the whole surface at this temperature, still beginning at the (533) plane, but being unable to traverse the (320) plane, as was the case at higher temperatures. The effect of decreasing the H_2 pressure is similar, in that it can also decrease the ability of the wave to cross over the (320) area.

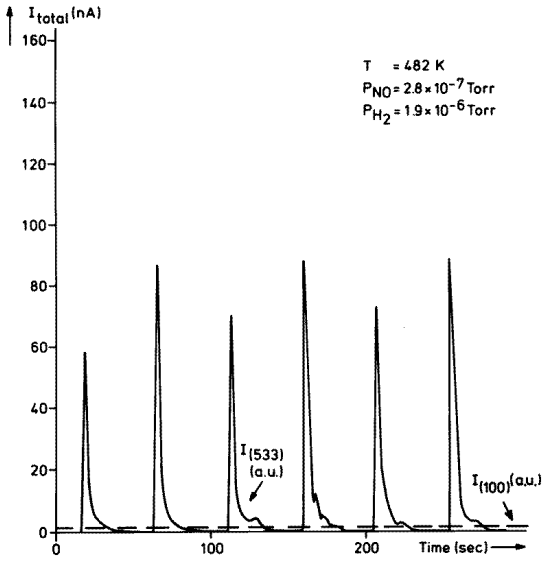

Figure 5. The variation of the emission current from the (533) and (100) planes as a function of time during the oscillatory behaviour of the NO–H_2 reaction on a Rh field emitter at 482 K, $p(\mathrm{NO}) = 3.6 \times 10^{-7}$ mbar and $p(\mathrm{H_2}) = 2.5 \times 10^{-6}$ mbar (from reference [37]).

The range of NO/H_2 ratios over which oscillations can be found extends from 2:3 to 1:50 [65]. On increasing the H_2 pressure the temperature at which oscillations occurred decreased [60, 65]. Using a scanning field electron microscope (SFEM) it is possible to selectively measure electrons originating from a specific single-crystal plane. In figure 5, the measured currents from the (533) and (100) planes are displayed under oscillatory conditions. The (100) surface is clearly not participating in the oscillation. Another surface that does not appear to participate in the oscillations from FEM work is Rh (210) [60]. Under certain experimental conditions it was also possible to observe the communication between

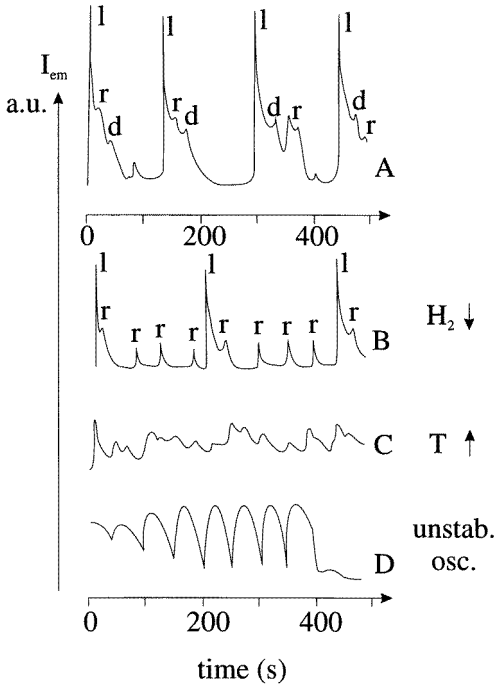

Figure 6. Variations of the emission current of a Rh tip under different experimental conditions. Trace A: regular oscillation at 432 K, $p(\mathrm{NO}) = 1\times10^{-7}$ mbar and $p(\mathrm{H_2}) = 1.3\times10^{-6}$ mbar; l, r and d represent surface waves initiated on the left, right and defect areas of the twin tip. Trace B: the effect of a decrease in the hydrogen pressure compared to trace A; $p(\mathrm{H_2}) = 9\times10^{-7}$ mbar. Trace C: the effect of temperature increase with respect to trace B, at 445 K. Trace D: unstable oscillations obtained after a quick temperature drop from 485 to 470 K at $p(\mathrm{NO}) = 1\times10^{-7}$ mbar and $p(\mathrm{H_2}) = 1.3\times10^{-6}$ mbar.

adjacent single-crystal tips [47]. This was realized through the preparation of a peculiar Rh tip, with [111]-oriented twins separated by a (100) plane. This central (100) plane was divided into two unequal parts by an extended one-dimensional region with defects, a grain boundary. This not only allowed an investigation into the synergetic behaviour of two adjacent single-crystal particles, but also into the role of a grain boundary and defects in the oscillatory processes. Once again, on heating in a flow of NO and H_2, the sudden increase in emission as previously described occurred at ∼465 K. On lowering the temperature, sustained oscillations were found, and can be categorized into several types [47].

(a) Oscillations that can be described as being local in nature were obtained after cooling the tip slowly to 450 K in a flow of NO and H_2. The increase in emission begins at the grain boundary and moves in both directions to the adjacent (310) planes, stopping at the (321) plane. As a result of this, a large part of the two tips does not get to participate in the oscillatory wave, such as the bright areas around the (111) surfaces.

(b) Regular oscillations extending across the whole twin-tip area, including these latter planes of high emission, could be obtained by further decreasing the temperature to 432 K. Under such conditions, the wave can spread from either of the tips to its neighbour, crossing the grain boundary.

(c) Regular oscillation, where the two tips are behaving independently of each other,

can be realized by a slight decrease in the H_2 pressure in comparison to that in (b). Here the oscillatory wave is not sufficiently 'strong' to cross the grain boundary. As with previous experiments, the wave began from the (533) surface, and moves initially to the (310) surface.

(d) If the temperature was subsequently increased, irregular behaviour was observed, in the form of a large number of centres that could trigger the wave. This and other types of oscillation mentioned here are illustrated in figure 6, by way of the variation of the emission current at constant voltage.

(e) Finally, unstable oscillations were also observed as the bright area around one of the (111) areas continuously changes size. These were realized by quickly dropping the temperature from 485 to 470 K. This behaviour stopped after a few cycles.

The FEM results obtained with the twin tip demonstrated the importance of defects as acting as active centres for the seeding of oscillatory processes on Rh. To summarize the NO–H_2 reaction over Rh field emitters, defects play a major role in the seeding of the oscillatory process, whether in the form of a highly stepped surface such as (533), or a grain boundary. This is also seen in macroscopic studies of large Rh single crystals [66–68]. The Rh(111) surface shows macroscopic rate oscillations, which when compared to those for Rh(533) were not only much smaller, but also less synchronized. The introduction of defects to the surface increased both the amplitude and the synchronization of the oscillations. The temperature range in which oscillations were found spanned from 440 to 480 K, a similar but slightly lower temperature range than for single-crystal experiments [66–68]. These macroscopic studies have given more insight into the mechanism of this reaction, which is discussed in section 6.

It is also necessary to take into account possible changes in surface structure of the tip when considering the mechanism for the observed oscillatory behaviour. Under the action only of NO, a Rh tip has been seen to undergo strong morphological changes as measured by FIM [69]. After exposing a Rh tip to ∼400 L NO at 520 K, the number of high-index planes on a [100]-oriented tip between the central (100) and peripheral (111) and (110) planes was greatly reduced [69]. The processes were thermally activated, and no morphological changes were seen for NO exposures at temperatures below 460 K [69].

5.2. Hysteresis in NO reduction reactions over Rh

A telltale sign of non-linear reaction is a hysteresis in reactivity when varying one parameter, such as temperature or pressure, while keeping other parameters constant. The NO reduction with NH_3 is such a reaction [70]. For NO:NH_3 ratios between 1:1 and 1:4 in the 10^{-6} mbar total pressure range, a hysteresis exists in the emission current at constant voltage between heating and cooling the sample. This was in fact another reaction that also showed oscillations in the field emission mode [71]. The oscillations were confined to a very small area of the tip, namely the (511)–(711) areas, and a rather narrow parameter range. In a flow on 1.3×10^{-7} mbar NO and 3×10^{-7} mbar NH_3, when the Rh tip was rapidly heated to a high temperature and then slowly cooled to 596 K, the emission intensities from the aforementioned planes started to periodically increase and decrease in phase with each other.

The NO–CO reaction over Rh did not show any hysteresis in emission current in the temperature range (<600 K) and pressure ranges ($<10^{-5}$ mbar) studied in the field emission mode [70]. Indeed no oscillations were observed on this metal in the parameter range used. Oscillations in the NO–CO reaction have been observed over a Rh(110) single crystal, but only at much higher pressures and temperatures [72].

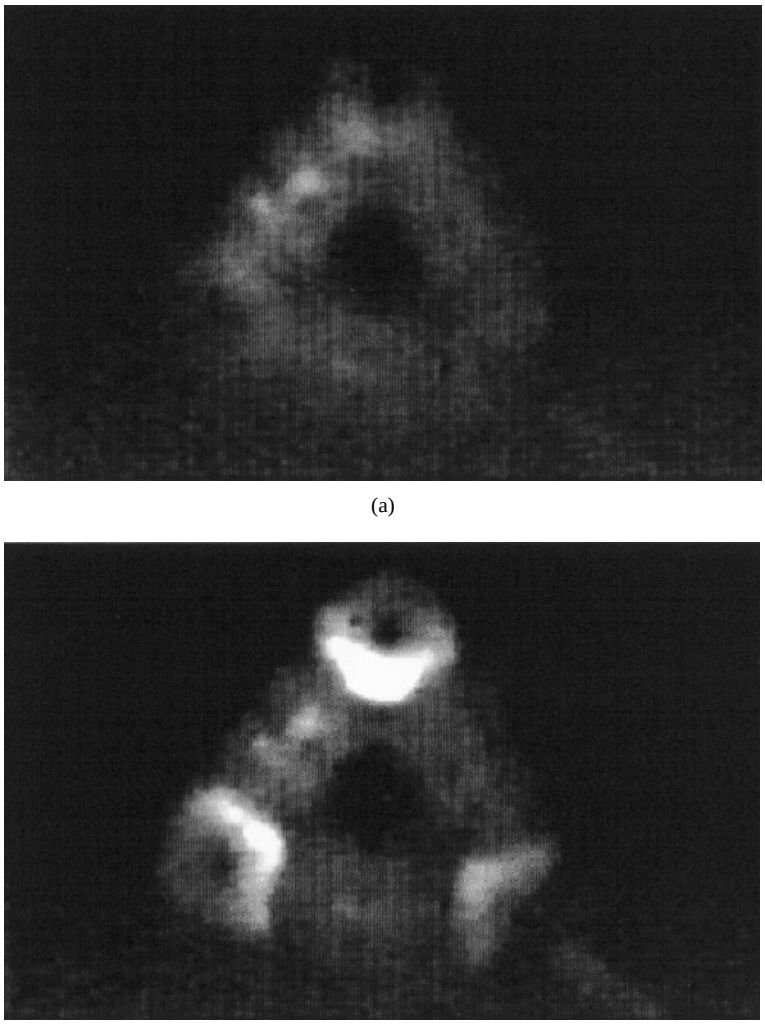

(a)

(b)

Figure 7. FEM images observed for the NO–H_2 reaction over a Pt field emitter at 416 K, $p(\mathrm{NO}) = 1 \times 10^{-5}$ mbar and $p(\mathrm{H_2}) = 1 \times 10^{-5}$ mbar. The images were recorded at (a) 0 s, (b) 5 s.

5.3. Non-linearity in NO reduction reactions over other Pt-group metals

In the case of a Pt tip, the NO–H_2 reaction also showed transient oscillations in the field emission mode [73], as well as sustained oscillations in the field-ion mode [74]. For example, in a flow of 1×10^{-5} mbar NO and 1×10^{-5} mbar H_2, heating a Pt tip led to an increase in the emission of all of the stepped surface around the (100) plane, but not the (100) plane itself [73]. This increase in emission began at 430 K, but this ring feature disappeared again at higher temperatures. On cooling, the ring was seen to reappear again periodically at 416 K every 70 ± 10 s. This behaviour was only transient and was never seen to last for more than 20 cycles, although the results could be reproduced again by heating and cooling the sample. Figure 7 shows the form of these transient oscillations, in which all

of the stepped areas around all three of the (100) planes present on this (111)-oriented tip are oscillating in phase with each other. Under different conditions, these separated active areas could oscillate either in or out of phase with each other [73]. The sustained oscillations found in the field-ion mode were found under different conditions, and were different in character to those found in the field emission mode [74]. The oscillations took the form of an increase in ion current starting at the (210) planes that spread rapidly towards the (100) plane. This increase in ion current remained active for only 0.1–0.2 s, and returned with a period of some 10 s [74].

Similar behaviour to that for Pt has also been observed for Ir field emitters, in the field emission mode, but with the central (100) plane also participating in the oscillation [75]. Additionally, the oscillations observed in this case were sustained, require an excess of H_2, and occurred at lower temperatures. The importance of surface diffusion in synchronizing surface oscillators in this case is also demonstrated, because at these lower temperatures, the (100) areas on tips where more than one (100) area was present oscillated asynchronously [75]. The very similar oscillatory behaviour seen for Pt, which occurred at higher temperatures, had the individual oscillators acting in phase with each other [73].

6. Non-linear behaviour of the NO–H_2 reaction over large Rh surfaces

6.1. Kinetic rate oscillations

The FEM results [60, 64, 65] clearly show that not all of the surfaces present on a Rh tip take part in the wave. In particular, the stepped (111) surfaces and the stepped (110) surfaces participate in the propagating reaction front whereas the Rh(100) surface does not take part in the reaction front at all [65]. Van Tol *et al* [65] suggested that on the Rh(100) surface a strongly bound non-reactive N_{ads} layer is formed. The oscillating waves have been interpreted in terms of an autocatalytic model [47, 60, 64, 65].

Based on the FEM studies reported by van Tol *et al* a number of large Rh single-crystal surfaces (0.5 cm^2) consisting of (111) and (100) terraces were selected by Janssen *et al* [67, 68, 76] and Cobden *et al* [66].

Rate oscillations in the rate of N_2 formation were observed over some of the selected Rh surfaces under similar experimental conditions to those for the FEM studies. All of these surfaces have in common that they consist of (111) structures. The same structure sensitivity was observed as in the FEM study by van Tol *et al* [65]. For example, the stepped Rh(533) shows oscillatory behaviour whereas Rh(100) is not active under similar conditions [67]. In addition, not only the activity but also the selectivity towards N_2 and NH_3 oscillates in time [68]. By changing the step density on the (111)-like surfaces, information was obtained about the effect of terrace width on the oscillatory behaviour. The NO–H_2 reactions over Rh(533), Rh(311) and Rh(111) behave quite similarly to one another.

Figure 8 shows oscillatory behaviour during the NO–H_2 reaction over Rh(533) with p(NO) of 0.8×10^{-6} mbar and a H_2/NO ratio of about 15 at around 490 K. Clearly, the selectivity towards N_2 and NH_3 oscillates in time: the rate of N_2 formation ($r(N_2)$) is out of phase with the rate of formation of NH_3 ($r(NH_3)$). H_2O is also a major reaction product, and $r(H_2O)$ is in phase with $r(NH_3)$. No N_2O is formed. Hence, reaction (1c) does not occur under the experimental conditions used.

The NO pressure also oscillates in time and this is a result of consumption of NO during the reaction. The overall time-average conversion of NO during rate oscillations is below 10%. The NO signal is out of phase with the NH_3 and H_2O signals [68] (not shown here). This indicates that at a high consumption of NO, i.e. at a low NO signal in the gas phase,

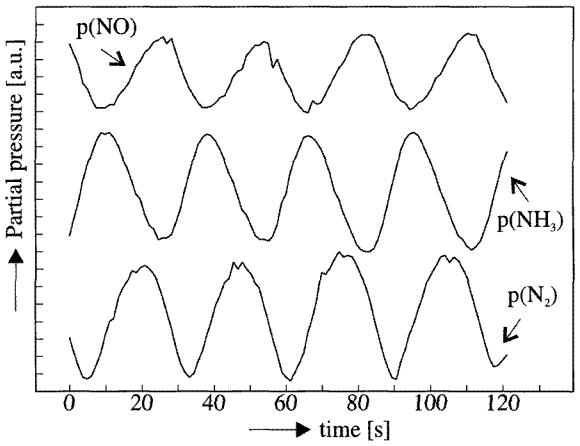

Figure 8. NO–H_2/Rh(533); the NH_3, NO and N_2 partial pressures as function of time with $p(\mathrm{NO}) = 0.8 \times 10^{-6}$ mbar, $H_2/\mathrm{NO} = 14.5$, $T = 494$ K. Note that in this figure the mass spectrometer signals have been shifted vertically.

the H_2O and NH_3 formation rates are high. Therefore, a direct relation exists between the conversion of NO and the formation rates of H_2O and NH_3. No such relation exists between $p(\mathrm{NO})$ and $r(N_2)$ in the oscillatory regime: the NO and N_2 signals are nearly in phase. Apparently, the N_{ads} atoms formed by the decomposition of NO remain on the surface before they react to form gaseous N_2 whereas O_{ads} is immediately released as H_2O into the gas phase.

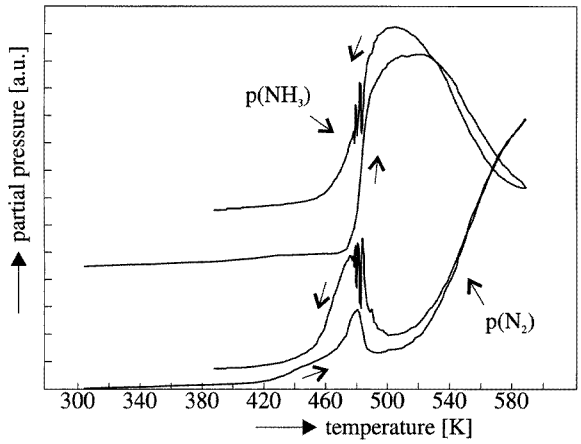

Figure 9. NO–H_2/Rh(533); the rate of N_2 and NH_3 formation as a function of temperature at $p(\mathrm{NO}) = 0.8 \times 10^{-6}$ mbar and $H_2/\mathrm{NO} = 15$; the heating and cooling rate is 0.10 K s^{-1}.

The rate oscillations are obtained by heating and cooling the surface in a reactant mixture until a transient region is reached. This region is coupled to a hysteresis in $r(N_2)$ as figure 9 illustrates for the NO–H_2 reaction over Rh(533). The formation of NH_3 is also displayed in figure 9. The figure indicates that $r(NH_3)$ and $r(N_2)$ are competitive processes, in particular

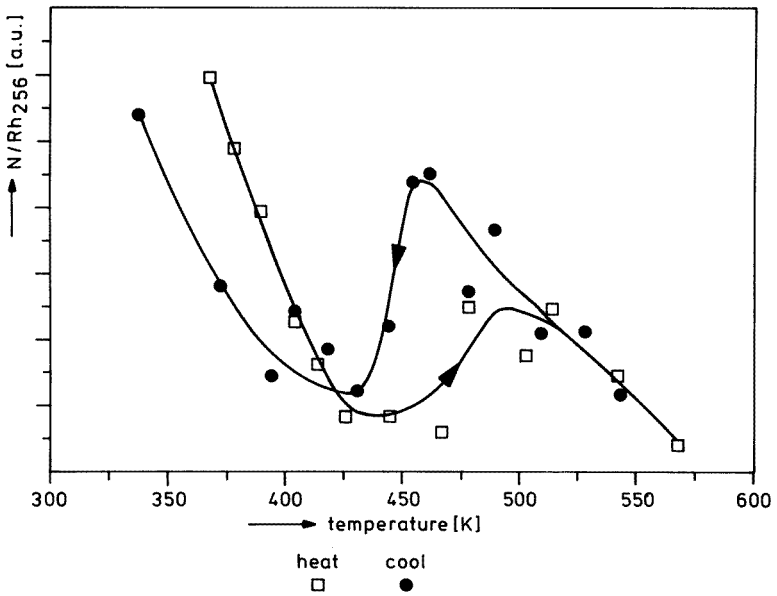

(a)

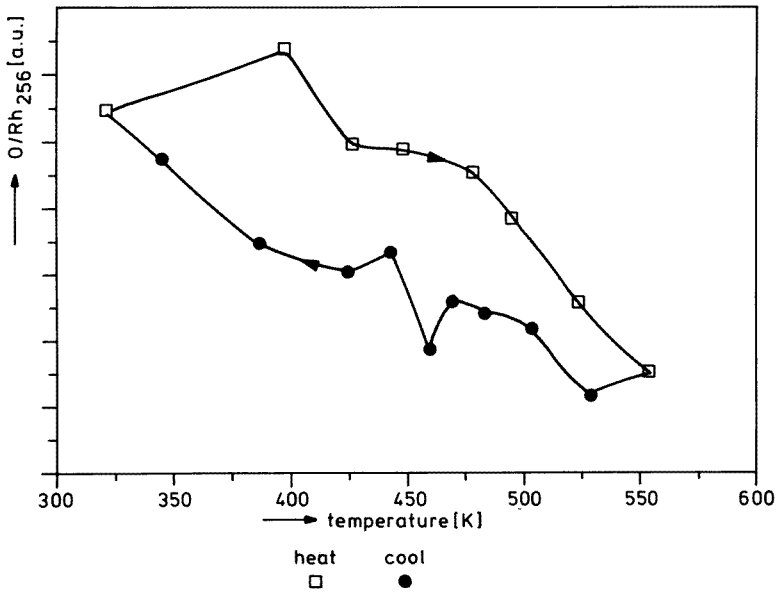

(b)

Figure 10. NO–H_2/Rh(533); (a) the N_{381}/Rh_{256} AES signal ratio upon heating (□) and upon cooling (●) at $p(NO) = 7.2 \times 10^{-8}$ mbar at a H_2/NO ratio of 14.5 and (b) the O_{510}/Rh_{256} AES signal ratio upon heating (□) and cooling (●) at $p(NO) = 7.2 \times 10^{-8}$ mbar and a H_2/NO ratio of 15.3.

in the transient region. That is, $r(N_2)$ and $r(NH_3)$ are out of phase, similarly to the observed phase relationship under oscillatory behaviour (figure 8). Under steady-state conditions, the H_2O formation rate (not shown) is the sum of $r(N_2)$ and $r(NH_3)$ [66]. At constant H_2/NO with decreasing NO pressure, the temperature at which oscillations appeared also decreased, whereas the period of the oscillations increased. For example, with a H_2/NO ratio of about 15 and a change in p(NO) from 8×10^{-7} mbar to 3×10^{-7} mbar, the period increased from about 30 to about 80 seconds [67].

In the oscillatory regime the H_2/NO ratio could be varied within a small range: between 12.3 and 16 at the given conditions for the experiments shown in figure 9. Within the small range of H_2/NO ratios the period of the rate oscillations did not change; outside the range the oscillations became irregular and finally they disappeared. No period doublings were observed by changing $p(H_2)$ within the narrow range of H_2/NO ratios where oscillations existed, as has been reported for the NO–H_2 reaction over Pt(100) by Siera *et al* [36]. Interestingly, when $p(H_2)$ was increased during the oscillations, initially the N_2 production rate decreased, and the NH_3 production rate increased and vice versa. The same phenomena could be observed when p(NO) was decreased but in the opposite direction. After some time (less than four periods) the system restores its original time-average activity level. Apparently, the rate oscillations are highly sensitive to changes in the partial pressures of the reactants. Therefore, it is concluded that gas-phase coupling plays an important role in the synchronization process of individual oscillators on the surface [12]. The observed orders in H_2 and NO for $r(N_2)$ and $r(NH_3)$ suggest that during rate oscillations the kinetics continuously switches between a positive and negative order in H_2 for N_2 formation.

6.2. The mechanism of the NO–H_2 reaction over Rh

In situ AES measurements have revealed that an N species accumulates on the surface between 450 and 500 K on the cooling branch (figure 10(a)) whereas the O AES peak intensity is relatively low in this temperature range (figure 10(b)). N_{ads} and NH_{ads} [77] are the most likely candidates to account for the increase in N AES intensity on the cooling branch in excess of H_2. The coverage of NO is assumed to be negligible at temperatures where the hysteresis in $r(N_2)$ is observed since NO dissociation proceeds with a high rate over Rh surfaces above 300 K provided that enough vacancies are present [18, 21, 78]. Moreover, the N species accumulates on the surface at temperatures above the desorption temperature of NO from Rh(533) [79]. The accumulation of N_{ads} is in line with the observed increase in $r(N_2)$ on the cooling branch since the local maximum in the N AES peak intensity coincides with the N_2 hysteresis peak. N_{ads} accumulates according to the following overall reaction:

$$NO + H_2 \rightarrow N_{ads} + H_2O. \tag{13}$$

N_2 is formed via the combination of two adsorbed N_{ads} atoms (process (5)).

The rate limiting step for N_2 formation is the combination of two N_{ads} atoms and it is determined by the stability of N_{ads} on the surface as confirmed by AES data (figure 10). Under the conditions used in the AES measurement the onset temperature for N_2 formation is around 500 K. Probably, densely packed N_{ads} islands are needed to favour N_2 formation since N_{ads}–N_{ads} interactions are repulsive as a TPD study revealed [79]. Repulsive N_{ads}–N_{ads} interactions have also been observed by Belton *et al* [25] and Borg *et al* [21] for N_{ads} on Rh(111). At H_2/NO ratios below 8, however, the onset temperature for N_2 formation is not determined by the N_{ads} combination step but it is limited by removal of O_{ads} [66], and the onset temperature for N_2 formation shifts to higher temperatures [68].

As figure 10 indicates, N_{ads} also accumulates on the heating branch just before the onset temperature of N_2 formation. The N_{ads} atoms accumulate at higher temperatures with respect to N_{ads} accumulation on the cooling branch. This is due to the fact that on the heating branch higher temperatures are needed to remove O_{ads} from the surface using H_2. The adsorption of H_2 can be suppressed by O_{ads}. At a certain temperature hydrogen adsorption becomes possible by the creation of vacancies on the surface, perhaps via some desorption of N_{ads} or some subsurface diffusion of O_{ads} or N_{ads} or removal of O_{ads} with H_{ads} at defect sites. The H_{ads} formed reacts with O_{ads} to form H_2O and the O AES intensity decreases rapidly, and N_{ads} atoms accumulate.

It has been suggested by Cobden *et al* [66] based on *in situ* AES measurements that O_{ads} accelerates the formation of N_2 due to repulsive N_{ads}–O_{ads} interactions. The small increase in $r(N_2)$ is accompanied with accumulation of O_{ads}. Repulsive N_{ads}–O_{ads} interactions have also been observed previously by Belton *et al* [25] for Rh(111) and by Comelli *et al* [80] for Rh(110).

The formations of NH_3 and H_2O both require a relatively large concentration of vacancies on the surface to dissociate NO and H_2 rapidly according to the following overall reactions: for NH_3:

$$N_{ads} + 3H_{ads} \rightarrow NH_3 + 4\square \tag{14}$$

and for H_2O:

$$O_{ads} + 2H_{ads} \rightarrow H_2O + 3\square \tag{15}$$

where $\square$ denotes a vacant active site on the surface.

Equations (14) and (15) show that for the formation of NH_3 relatively more H_2 is needed than for the formation of H_2O. The lifetime of H_{ads} on Rh surfaces is very small since it is known from TDS studies reported in literature that H_2 desorbs below 350 K from Rh surfaces [81]. Hence, its concentration can be considered to be small. Compared to O_{ads} and N_{ads}, H_{ads} is very mobile on Rh surfaces [82].

The formation of NH_3 proceeds via the formation of an NH_{ads} intermediate as has been observed by Tanaka *et al* [77] by means of HREELS for Rh(100). Their study shows that NH_{ads} disappears from the surface when hydrogen is removed from the gas phase at 475 K [83]. Wagner and Schmidt [84] reported that NH_{ads} on Rh(111) is stable up to 430 K under TDS conditions and the relative adsorption bond strengths of the hydrogenated $NH_{x,ads}$ ($x = 1$–3) are as follows: $NH_{ads} > NH_{2,ads} > NH_{3,ads}$. Therefore, the maximum observed in $r(NH_3)$ is attributed to the stability of NH_{ads} (figure 9).

The hydrogenation of O_{ads} to H_2O is generally believed to be a fast process on Rh surfaces. Provided that enough vacancies are present this reaction proceeds already at room temperature as has been reported for Rh(111) [84, 85] and for a Rh field emitter [86]. The concentration of OH_{ads} as an intermediate for the formation of H_2O is therefore neglected. The formation of H_2O can thus be described with the overall reaction (15). Thermal desorption studies of H_2O from Rh(111) show that H_2O desorbs below 200 K [87] and as a result H_2O immediately leaves the surface once it is formed. The same argument also holds for NH_3 [84]. No maximum in the H_2O production was observed in the measured temperature range as was observed for NH_3 formation, since also when N_2 is formed H_2O is produced as well (equation (13)).

6.3. The oscillatory model

The model proposed [68] to describe the rate oscillations and the observed product distribution as a function of time during oscillatory behaviour belongs to the category IIc

(see section 3). A relatively large concentration of vacancies will favour the dissociation rates of NO and H_2 and the formed N_{ads} and O_{ads} atoms are hydrogenated to yield NH_3 and H_2O. Accordingly, an increase in $p(H_2)$ will favour NH_3 formation (positive order). For the formation of N_2, however, accumulation of N_{ads} is needed and as a result the consumption rates of NO and H_2 decrease relatively due to a decrease in available vacant sites.

In conclusion, in the regime where rate oscillations occur the surface composition switches continuously between a N_{ads}-rich and an O_{ads}/NH_{ads} layer. The following oscillatory cycle can be proposed:

(I) N_{ads} atoms accumulate on the surface via the overall reaction (13). The dissociation rate of NO is suppressed and the selectivity towards N_2 is enhanced due to N_{ads} island formation.

(II) Hydrogen adsorption becomes suppressed since the concentration of vacancies drops and O_{ads} atoms accumulate on the surface. Due to repulsive O_{ads}–N_{ads} interactions the rate of N_2 formation is enhanced further.

(III) The removal of N_{ads} is faster than the N_{ads} accumulation rate and, consequently, the NO dissociation rate and the H_2 dissociation increase. NH_3 and H_2O formation are favoured over N_2 formation.

(IV) Due to the removal of O_{ads}, N_{ads} atoms are able to accumulate and stage I is reached again.

Several questions concerning the oscillatory cycle are still unanswered. For example, it is not understood in detail what is driving the N_{ads} coverage to oscillate and, in particular, what factors determine the transitions between stages III and IV. Theoretical modelling by Makeev *et al* [88] suggests that repulsive interactions between possible intermediates like NO_{ads}, N_{ads}, NH_{ads} and O_{ads} create the non-linearity in the reaction rate.

Rate oscillations have not been found during the NO–CO and NO–NH_3 reaction over Rh(111), Rh(533) and Rh(311) under similar conditions to those for the NO–H_2 reaction. No hysteresis in $r(N_2)$ due to accumulation of N_{ads} atoms was observed for these reactions. Temperatures higher than 500 K are needed for the formation of N_2 and this is related to the desorption temperature of CO from Rh surfaces [89] and to the steady-state decomposition of NH_3 at around 500 K.

6.4. The role of surface structure

A key step in the oscillating mechanism is the reversible accumulation of N_{ads}. TDS shows that N_{ads} atoms start to combine and desorb between 450 and 600 K from Rh(533) [67]. In contrast, Rh(100) is deactivated in this temperature range due to the formation of a $c(2 \times 2)$–N adlayer that is stable up to 700 K [67, 76, 77]. Strongly bound N_{ads} atoms also form on the four-atom wide (100) terraces of Rh(410) and Rh(711) and, accordingly, no rate oscillations were observed over these surfaces either.

The stability of N_{ads} on Rh(111) and Rh(311) is similar to that of N_{ads} on Rh(533) [21, 90, 79] and rate oscillations have been found over these three surfaces. The rate oscillations over Rh(533) and Rh(311) are more synchronized than those over Rh(111). Obviously, the ordered step structure present on Rh(311) and Rh(533) creates more regular rate oscillations. Increasing the concentration of defects on Rh(111) by means of Ar^+ bombardment, however, also resulted in enhancement of the synchronization of the oscillations over Rh(111) [66].

Major surface reconstructions like facetting are not believed to play a role in the oscillating mechanism. An *in situ* LEED study confirmed the absence of a new surface structure on Rh(111) above 400 K. Below 400 K a (2×2) structure was observed that

is attributed to the formation of an O_{ads} layer [91]. Nevertheless, N- and O-induced reconstructions of Rh(311) and Rh(533) are likely processes. For example, it is known that Rh(110), having a structure that resembles that of Rh(311), reconstructs during the NO–H_2 reaction at relatively low temperatures [92–95]. The reconstructions were monitored by Mertens and Imbihl [96] by means of *in situ* LEED. Rate oscillations have also been observed [96] in $r(N_2)$ and p(NO) at 550 K for excess of H_2 with NO in the 10^{-6} mbar pressure regime. The similar non-linear behaviour of the stepped (111) and stepped (110) surfaces during the NO–H_2 reaction was already observed by van Tol *et al* [65] in their FEM studies. In addition, the stability of N_{ads} on Rh(110) is similar to that of N_{ads} on Rh(111), Rh(533) and Rh(311) [97, 98].

7. Spatiotemporal processes

The chemical waves observed by Mertens and Imbihl [96, 99] for NO–H_2 on Rh(110) by means of PEEM form a new type among the known ones. The Rh(110) surface structure does not remain fixed under NO–H_2 reaction conditions but the structure and composition change continuously leading to a state-dependent anisotropy of the wave patterns. The changes in surface structure are caused by N- and O-induced reconstructions. Elliptical and rectangular shapes have been observed by Mertens and Imbihl [99] and these shapes could be controlled by changing the experimental parameters such as temperature, p(NO) and $p(H_2)$. The shapes have also been modelled by Imbihl *et al* [96]. N_{ads} and H_{ads} have been proposed to be the species that diffuse over the surface whereas O_{ads} remains immobile [99].

PEEM has also been applied to study spatiotemporal pattern formation over Rh(111) [91]. The main purpose of this study was to link the data obtained with FEM (see section 5) with the macroscopic Rh single-crystal surfaces described in section 6. Furthermore it was hoped to gain more insight into the role of steps in the synchronization process. Chemical waves have been observed in a temperature regime (width about 30 K) that is located on the low-temperature side of the oscillatory region and the N_2 hysteresis peak. In this region the formation rates of N_2, NH_3 and H_2O are very low. The results obtained with Rh(111) are very similar to those for Rh(110) [99] except that no square chemical waves were observed. In general, when one diffusing species is involved and when the velocity of the fronts is the same in all directions circular patterns will be observed [9, 12] as is the case for Rh(111) [91]. Structural defects are likely to be initiators of the chemical waves. In a FEM study by Cholach *et al* [47] it is reported that also a grain boundary on a Rh tip can act as a diffusional barrier for the propagating reaction front.

In the PEEM study a new species has been observed on Rh(111) characterized by a work-function drop below that of the clean surface when two or more reaction fronts collide [91]. This species has been tentatively attributed to subsurface oxygen. Figure 11 illustrates the formation of a spiral and the region with the reduced work function.

The PEEM investigation did not reveal the role of the steps in the synchronization mechanism. Gas-phase coupling due to pressure variations in the gas phase plays an important role for the macroscopic rate oscillations as the PEEM data indicate. At temperatures just below the oscillatory range surface diffusion becomes more dominant than gas-phase coupling and spatiotemporal pattern formation occurs. Local intensity measurements, however, reveal that the rate is still oscillating on a local scale (area $30 \times 30\ \mu m^2$). A very similar existence range for spatiotemporal pattern formation has been observed for other catalytic systems reported in the literature, e.g. for the NO–CO reaction over Pt(100) [52] and for the NO–NH_3 reaction over Pt(100) (reference [100]). In these systems the surface is usually spatially uniform when macroscopic rate oscillations are

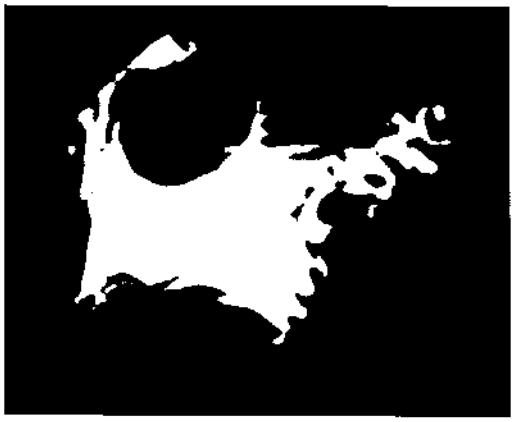

Figure 11. NO–H_2/Rh(111); development of the spiral and the region of reduced work function at 456 K with $p(\mathrm{NO}) = 1 \times 10^{-6}$ mbar and $H_2/\mathrm{NO} = 6.5$ (from reference [91]). The diameter of the image is about 600 μm.

observed in the gas phase. Since the macroscopic rate oscillations over Rh(111), Rh(311) and Rh(533) are not perfectly synchronized it is expected that these surfaces are not spatially uniform during rate oscillations. Local bright fronts have been observed by means of PEEM in the oscillatory region, and the adsorbate layer changes in a very dynamic way.

Breakdown of gas-phase coupling has been observed in [52] due to the fact that at temperatures below the oscillatory region large defects start to emit waves that disturb the synchronization (reference [101]). Similar processes occur during the NO–H_2 reaction over Rh(111) and Rh(533). For example, spirals pinned to defects have been observed [91]. The fact that defects break down gas-phase coupling is in contrast with the observation that small defects and steps (<1 μm) enhance the synchronization. At present this process is not understood. It can be suggested, for example, that the small defects and the (100) steps keep the size of N_{ads} islands within a certain range, and hence that non-linear behaviour can be observed when N_{ads}–N_{ads} interactions are important. It can also be suggested that defects stimulate the formation of subsurface oxygen (O_{sub}). It is known from various reports in the literature that the more open and rough the Rh surfaces are, the better O_{ads} diffuses into the near-surface region (references [102–104]). O_{sub} could affect the bonding of adsorbed intermediates and, therefore, cause a non-linearity in the rate. This however, remains highly speculative.

8. General discussion

The topic of this review—non-linear behaviour of NO reduction reactions—has been discussed in detail in the relevant sections. Spatiotemporal processes have been observed for the NO–H_2 reaction with FEM, FIM and PEEM. Oscillations in rates and selectivities have been found on macroscopic Pt(100) and Rh surfaces with (111) terraces. The mechanisms of non-linear behaviour are very different for Pt and Rh. In this last section we shall limit ourselves to a brief discussion of general aspects: a comparison of FEM and PEEM results, the difference between Pt and Rh and, finally, the mechanism proposed for the non-linear behaviour, in particular for Rh surfaces.

Spatiotemporal processes were observed over Rh field emitters as discussed in section 5

and over Rh(110) [96, 99] and Rh(111) surfaces by PEEM [91] in the form of chemical wave patterns. The chemical nature of the wave seen in the NO–H_2 reaction over Rh field emitters cannot be unambiguously determined from the FEM results themselves, but with the help of single-crystal results can be greatly clarified. The increase in emission current beginning at the (533) plane could be attributed to either the formation of a work-function-decreasing reaction intermediate, or the removal of a work-function-increasing intermediate. The most likely explanation is that the dark surfaces are mainly N_{ads} covered, on which O_{ads} is built up, pushing N_{ads} from the surface as N_2, thus greatly increasing the amount of free space on the surface for H_2 dissociation, and hence H_2O and NH_3 production. The combination of high reaction rate (i.e. a large number of free reaction sites) and intermediates such as NH_{ads} (decreasing the work function) leads to an increase in emission current.

Under appropriate experimental conditions surface diffusion may play a more dominant role than gas-phase coupling. Gas-phase coupling is the major process for synchronization on large single-crystal surfaces in the 10^{-5} mbar range [46]. On the field emitter tip, surfaces communicate through surface reaction and diffusion. As a result a surface explosion on the heating branch was observed for Rh, i.e. a rapid increase in field electron emission intensity close to the onset temperature of the reaction. Such a surface explosion in activity has not been observed for large Rh single-crystal surfaces.

The waves observed by FEM take place over a wide range of H_2/NO ratios as opposed to the narrow range of H_2/NO ratios where macroscopic rate oscillations could be observed over the Rh single-crystal surfaces. This again illustrates the dominant role of surface diffusion in the chemical waves in the case of the Rh field emitter. Also in other catalytic systems that exhibit oscillatory behaviour and spatiotemporal pattern formation it is shown that macroscopic rate oscillations occur in a narrower range of experimental parameters (references [52, 100]).

The most striking observation in comparing the behaviour of the small tip and the behaviour of the large single-crystal surfaces is that spatiotemporal processes take place on a very small scale (20 Å) and on very large scale (1 μm). Due to the similarity of the waves observed on tips and large single crystals it is assumed that the natures of the fronts are the same. Therefore, it is concluded that the reaction fronts are not strongly affected by the size of the surface involved. The shape of the waves is determined by the geometry of the surface on the microscopic level. That is, FEM data indicate that the wave moves parallel to surface steps. In addition to the reaction fronts discussed, a different kind of spatiotemporal pattern formation is observed due to the larger size of the crystals. The fronts can develop in time and space and interact with each other leading to the formation of a new species, and the waves can interact with relatively large defects since spirals are observed [91].

8.1. Comparison with other isothermal oscillating systems

The proposed mechanism for the observed rate oscillations during the NO–H_2 reaction over Rh surfaces represents a new type among the known models that have been described in the literature for oscillations over single-crystal surfaces under isothermal conditions in the low-pressure regime ($p < 10^{-4}$ mbar). For example, although surface reconstructions induced by O and N may occur on Rh surfaces [91], it is not an essential step in the oscillatory mechanism. This is not the case for oscillations during CO oxidation over Pt(100) (references [105, 106]), Pt(210) (reference [107]) and Pt(110) (reference [108]) in which the surface reconstruction plays a major role. Over these Pt surfaces the oscillations in the rate of CO_2 formation are thought to be driven by a periodic surface reconstruction which modulates the oxygen sticking coefficient and, hence, the catalytic activity. Recently

this model was refined by Gruyters *et al* (reference [109]) based on new experimental data for the oxygen sticking coefficient and the non-linear growth rate of CO (1×1) islands. Over Pd(110) the CO oxidation also exhibits oscillatory activity under some experimental conditions (references [40, 110]). These oscillations are not driven by a periodic surface reconstruction but a feedback mechanism involving subsurface oxygen has been proposed. A slow formation/removal process of subsurface oxygen modulates the catalytic activity in a periodic manner. This model is related to the so-called 'oxide model' described by Sales *et al* [29] for some oscillatory catalytic systems under atmospheric pressures. However, for Pd(110) it is believed that the subsurface oxygen is different in nature from a real oxide (references [40, 110]). Recently, Bondzie *et al* (reference [111]) by using new experimental data have called this subsurface oxygen model into question. Subsurface oxygen can be formed on Rh surfaces but at the H_2-rich NO–H_2 mixtures for which the oscillations are observed over Rh this is not a likely process. Nevertheless, under certain experimental conditions slow rate oscillations have been reported for the CO–NO and D_2–NO reaction over Rh(110) by Kruse *et al* (references [78, 112]) at relatively high temperatures (900 K) due to a slow formation/reduction cycle of a Rh oxide. As a result, the reductant plays a minor role as opposed to the mechanism of the rate oscillations during the NO–H_2 reaction over Rh at low temperatures.

The model proposed in this study for the NO–H_2 reaction over Rh is in some way related to the vacancy model. The concentration of vacancies on the Rh surface does play an important role in the process but it is determined by the coverage of N_{ads} atoms on the surface and not by the coverage of molecular NO_{ads}. Therefore, several features of the oscillatory reduction of NO over Pt(100) and NO–H_2 reaction over Rh are strikingly different. For example, accumulation of N_{ads} on Pt(100) does not take place under reaction conditions [36]. Formation of small amounts of N_2O has been found during the rate oscillations of the NO–H_2 reaction [36] and the NO–NH_3 reaction over Pt(100) [56]. Variations in the coverage of molecularly adsorbed NO cause the selectivity to oscillate: $r(N_2)$, $r(H_2O)$ and $r(NH_3)$ are in phase and out of phase with $r(N_2O)$. Therefore, a positive order in H_2 for N_2 and NH_3 formation and a negative order in H_2 for N_2O formation was observed by Siera *et al* [36]. Since the dissociation of NO on Pt is strongly structure sensitive [49] the oscillatory behaviour of the catalytic reduction of NO over Pt surfaces is also structure sensitive [50, 73].

In conclusion the mechanism of the oscillatory behaviour of the NO–H_2 reaction over Pt(100) is different from that over Rh: over Pt(100) the dissociation of NO is rate limiting whereas over Rh the ability to accumulate N_{ads} in a reversible manner plays a central role.

Non-linear behaviour of surface reactions has become an active field of research in the past ten years. A variety of interesting and complex phenomena have been observed. It is anticipated that owing to further development of experimental methods and the increasing use of more advanced computer modelling our insights into the fascinating area of oscillatory surface reactions will increase in the next decade. New generations of STM could give information on variations in local surface structure during oscillations. There is an urgent need to analyse the species present on the surface during oscillations. Fast and non-destructive techniques are now available for this purpose.

It is anticipated that in the next decade one will be able to calculate the experimental conditions to find oscillatory behaviour caused by a particular mechanism for a given reaction on selected metal surfaces.

References

[1] Lotka A J 1920 *J. Am. Chem. Soc.* **42** 1595
[2] Field R J and Noyes R M 1974 *J. Chem. Phys.* **60** 1877
[3] Belousov B P 1959 *Ref. Radiats. Med.* **1958** 145
[4] Zhabotinskii A M 1964 *Dokl. Akad. Nauk. SSR* **157** 392
[5] van Tol M F H, Mergler Y L, Koutstaal C A and Nieuwenhuys B E 1994 *Nevacblad* **32** 93
[6] Razon L F R and Schmitz R A 1986 *Catal. Rev. Sci. Eng.* **28** 89
[7] Ertl G 1990 *Adv. Catal.* **37** 213
[8] Gray P and Scott S K 1990 *Chemical Oscillations and Instabilities* (Oxford: Clarendon)
[9] Imbihl R 1993 *Prog. Surf. Sci.* **44** 185
[10] Schüth F, Henry B E and Schmidt L D 1993 *Adv. Catal.* **39** 51
[11] Slinko M M and Jaeger N I 1994 Oscillating heterogeneous catalytic systems *Stud. Surf. Sci. Catal.* 86
[12] Imbihl R and Ertl G 1995 *Chem. Rev.* **95** 697
[13] Nieuwenhuys B E 1993 *Elementary Reaction Steps in Heterogeneous Catalysis (Nato ASI series C, vol 398)* ed R-W Joyner and R A van Santen (Dordrecht: Kluwer) p 155
[14] Kobylinski T B and Taylor B W 1974 *J. Catal.* **33** 376
[15] Taylor K C 1984 *Automotive Catalysis* (Berlin: Springer)
[16] Lambert R M and Comrie C M 1974 *Surf. Sci.* **46** 61
[17] Siera J, Rutten F and Nieuwenhuys B E 1991 *Catal. Today* **10** 353
[18] Wolf R M, Bakker J W and Nieuwenhuys B E 1991 *Surf. Sci.* **246** 135
[19] Hirano H, Yamada T, Tanaka K I, Siera J, Cobden P D and Nieuwenhuys B E 1992 *Surf. Sci.* **262** 97
[20] Hirano H, Yamada T, Tanaka K I, Siera J and Nieuwenhuys B E 1993 *Stud. Surf. Sci. Catal.* **75** 345
[21] Borg H J, Reijerse J F C J M, van Santen R A and Niemantsverdriet J W 1994 *J. Chem. Phys.* **101** 10 052
[22] Zemlyanov D Y, Smirnov M Y, Gorodetskii V V and Block J H 1995 *Surf. Sci.* **329** 61
[23] Permana H, Ng K Y S, Peden C H F, Schmieg S J and Belton D N 1995 *J. Phys. Chem.* **99** 16 344
[24] Belton D N, DiMaggio C L, Schmieg S J and Ng K Y S 1995 *J. Catal.* **157** 559
[25] Belton D N, DiMaggio C L and Ng K Y S 1993 *J. Catal.* **144** 273
[26] Chen C C, Wolf E E and Chang H C 1993 *J. Phys. Chem.* **97** 1055 and references therein
[27] Qin F, Wolf E E and Chang H C 1994 *Phys. Rev. Lett.* **72** 1459
[28] Lane S L and Luss D 1993 *Phys. Rev. Lett.* **70** 830
[29] Sales B C, Turner J E and Maple M D 1982 *Surf. Sci.* **113** 272
[30] Burrows U A, Sundaresan S, Chabal Y J and Christmann S B 1987 *Surf. Sci.* **180** 110
[31] Mergler Y and Nieuwenhuys B E 1996 *J. Catal.* **161** 292
[32] Adloch W, Lintz H G and Weisker T 1981 *Surf. Sci.* **103** 576
[33] Singh-Boparai S P and King D A 1980 *Suppl. Le Vide* **201** 403
[34] Fink T, Dath J-P, Bassett M R, Imbihl R and Ertl G 1991 *Surf. Sci.* **245** 96
[35] Schwartz S B and Schmidt L D 1988 *Surf. Sci.* **206** 169
[36] Siera J, Cobden P D, Tanaka K and Nieuwenhuys B E 1991 *Catal. Lett.* **10** 335
[37] Cobden P D, Siera J and Nieuwenhuys B E 1992 *J. Vac. Sci. Technol.* A **10** 2487
[38] Slinko M, Fink T, Löher T, Madden H H, Lombardo S J, Imbihl R and Ertl G 1993 *Stud. Surf. Sci. Catal.* **75** 1583
[39] Cutlip M B, Hawkins C J, Mukesh D, Morton W and Kenney C N 1983 *Chem. Eng. Commun.* **22** 329
[40] Bassett M R and Imbihl R 1990 *J. Chem. Phys.* **93** 811
[41] Eiswirth M and Ertl G 1995 *Chemical Waves and Patterns* ed K Showalter and R Kapral (Amsterdam: Kluwer) p 447
[42] Rausenberger R, Swiech W, Rastomjee C S, Mundschau M, Engel W, Zeitler E and Bradshaw A M 1993 *Chem. Phys. Lett.* **215** 109
[43] Smiech M, Rausenberger B, Engel W, Bradshaw A M and Zeitler E 1993 *Surf. Sci.* **294** 297
[44] Rotermund H H, Haas G, Franz R U, Tromp R M and Ertl G 1995 *Science* **270** 608
[45] Gorodetskii V V, Block J H, Drachsel W and Ehsasi M 1993 *Appl. Surf. Sci.* **67** 198
[46] Ehsasi M, Frank O, Block J H and Christmann K 1990 *Chem. Phys. Lett.* **165** 115
[47] Cholach A R, van Tol M F H and Nieuwenhuys B E 1994 *Surf. Sci.* **320** 281
[48] Gorte R J, Schmidt L D and Land J L G 1981 *Surf. Sci.* **109** 367
[49] Masel R I 1986 *Catal. Rev. Sci. Eng.* **28** 335
[50] Veser G and Imbihl R 1992 *J. Chem. Phys.* **96** 7155
[51] Leerkamp P, Wolf R M and Nieuwenhuys B E 1988 *J. Physique Coll.* **49** C6 11
[52] Veser G and Imbihl R 1994 *J. Chem. Phys.* **100** 8483

[53] Fink T, Dath J P, Imbihl R and Ertl G 1991 *J. Chem. Phys.* **95** 2109
[54] Hopkinson A, Bradley J M, Guo X C and King D A 1993 *Phys. Rev. Lett.* **71** 1597
[55] Hopkinson A and King D A 1995 *Chem. Phys. Lett.* **232** 1
[56] van Tol M F H, Siera J, Cobden P D and Nieuwenhuys B E 1992 *Surf. Sci.* **274** 63
[57] Lombardo S J, Fink T and Imbihl R 1993 *J. Chem. Phys.* **48** 5526
[58] Lombardo S J, Esch F and Imbihl R 1992 *Surf. Sci.* **271** L367
[59] Gruyters M, Pasteur A T and King D A 1996 *J. Chem. Soc. Faraday Trans.* **92** 2941
[60] van Tol M F H, Gielbert A and Nieuwenhuys B E 1992 *Catal. Lett.* **16** 297
[61] Ernst N, Bozdech G, Gorodetskii V V, Kreuzer H-J, Wang R I C and Block J H 1994 *Surf. Sci.* **318** L1211
[62] Gorodetskii V V, Lauterbach J, Rotermund H-H, Block J H and Ertl G 1994 *Nature* **370** 276
[63] Hendrickx H A C M, Winkelman A M E and Nieuwenhuys B E 1987 *Appl. Surf. Sci.* **27** 458
[64] van Tol M F H, Gielbert A and Nieuwenhuys B E 1993 *Appl. Surf. Sci.* **67** 179
[65] van Tol M F H, Wouda P T and Nieuwenhuys B E 1994 *J. Vac. Sci. Technol.* A **12** 2176
[66] Cobden P D, Janssen N M H, van Breugel Y and Nieuwenhuys B E 1996 *Surf. Sci.* **366** 432
[67] Janssen N M H, Nieuwenhuys B E, Ikai M, Tanaka K and Cholach A R 1994 *Surf. Sci. Lett.* **319** L29
[68] Janssen N M H, Cobden P D, Nieuwenhuys B E, Ikai M, Mukai K and Tanaka K 1995 *Catal. Lett.* **35** 155
[69] Voss C and Kruse N 1994 *Appl. Surf. Sci.* **87+88** 134
[70] van Tol M F H 1993 *PhD Thesis* Leiden University, The Netherlands
[71] van Tol M F H, de Maaijer-Gielbert A and Nieuwenhuys B E 1993 *Chem. Phys. Lett.* **205** 207
[72] Schmatloch V and Kruse N 1992 *Surf. Sci.* **269+270** 488
[73] Cobden P D, Cholach A R and Nieuwenhuys B E, unpublished results
[74] Voss C and Kruse N 1994 *Appl. Surf. Sci.* **87+88** 127
[75] Cobden P D, Janssen N M H, van Breugel Y and Nieuwenhuys B E 1996 *Faraday Discuss.* **105** and to be submitted
[76] Janssen N M H, Neill J A, Cobden P D and Nieuwenhuys B E 1995 *Proc. 2nd Conf. on Unsteady State Processes in Catalysis (St Louis, MO)*
[77] Tanaka K, Yamada T and Nieuwenhuys B E 1991 *Surf. Sci.* **242** 503
[78] Schmatloch V, Jirka I, Heinze S and Kruse N 1995 *Surf. Sci.* **331–333** 23
[79] Janssen N M H *et al* 1997 in preparation
[80] Comelli G, Lizzit S, Hofmann P, Paolucci G, Kiskinova M and Rosei R 1992 *Surf. Sci.* **277** 31
[81] Gorodetskii V V, Nieuwenhuys B E, Sachtler W H M and Boreskov G K 1981 *Surf. Sci.* **108** 225
[82] Seebauer E G, Kong A C F and Schmidt L D 1988 *J. Chem. Phys.* **88** 6587
[83] Yamada T, Hirano H, Tanaka K, Siera J and Nieuwenhuys B E 1990 *Surf. Sci.* **226** 1
[84] Wagner M L and Schmidt L D 1995 *J. Phys. Chem.* **99** 805
[85] Yates Y T, Thiel P A and Weinberg W H 1979 *Surf. Sci.* **82** 45
[86] Gorodetskii V V, Nieuwenhuys B E, Sachtler W H M and Boreskov G K 1981 *Appl. Surf. Sci.* **7** 335
[87] Wagner F T and Moylan T E 1987 *Surf. Sci.* **191** 121
[88] Makeev A G, Slinko M M, Janssen N M H, Cobden P D and Nieuwenhuys B E 1996 *J. Chem. Phys.* **105** 7210
[89] Gorodetskii V V and Nieuwenhuys B E 1981 *Surf. Sci.* **105** 299
[90] Root T W, Schmidt L D and Fisher G B 1983 *Surf. Sci.* **134** 30
[91] Janssen N M H, Schaak A, Nieuwenhuys B E and Imbihl R 1996 *Surf. Sci.* **364** L555
[92] Murray P W, Thornton G, Bowker M, Dhanak V R, Baraldi A, Rosei R and Kiskinova M 1993 *Phys. Rev. Lett.* **26** 4369
Murray P W, Leibsle F M, Thornton G, Bowker M, Dhanak V R, Baraldi A, Kiskinova M and Rosei R 1994 *Surf. Sci.* **304** 48
[93] Dhanak V R, Baraldi A, Rosei R, Kiskinova M, Murray P W, Thornton G and Bowker M 1994 *Phys. Rev.* **50** 8807
[94] Dhanak V R, Baraldi A, Comelli G, Prince K C, Rosei R, Atrei A and Zanazzi E 1995 *Phys. Rev.* B **51** 1965
[95] Gierer M, Mertens F, Over H, Ertl G and Imbihl R 1995 *Surf. Sci.* **339** L903
[96] Mertens F M 1995 *PhD Thesis* Freie Universität Berlin
Mertens F and Imbihl R 1996 *Surf. Sci.* **347** 355
[97] Baird R J, Ku R C and Wynblatt P 1980 *Surf. Sci.* **97** 346
[98] Kiskinova M, Lizzit S, Comelli G, Paolucci G and Rosei R 1993 *Appl. Surf. Sci.* **64** 185
[99] Mertens F and Imbihl R 1994 *Nature* **370** 124
[100] Veser G, Esch F and Imbihl R 1992 *Catal. Lett.* **13** 371
[101] Mertens F, Imbihl R and Mikhailov M 1993 *J. Chem. Phys.* **99** 8668

[102] Belton D N, Fisher G B and DiMaggio C L 1990 *Surf. Sci.* **233** 12
[103] Rebholz M, Prins R and Kruse N 1992 *Surf. Sci.* **269/270** 293
[104] Janssen N M H, van Tol M F H and Nieuwenhuys B E 1994 *Appl. Surf. Sci.* **74** 1
[105] Ertl G, Norton P R and Rüstig J 1982 *Phys. Rev. Lett.* **49** 177
[106] Imbihl R, Cox M P and Ertl G 1985 *J. Chem. Phys.* **83** 1578
Imbihl R, Cox M P and Ertl G 1986 *J. Chem. Phys.* **84** 3519
[107] Sander M, Imbihl R and Ertl G 1991 *J. Chem. Phys.* **95** 6162
[108] Eiswirth M and Ertl G 1986 *Surf. Sci.* **177** 90
[109] Gruyters M, Ali T and King D A 1995 *Chem. Phys. Lett.* **232** 1
[110] Ladas S, Imbihl R and Ertl G 1989 *Surf. Sci.* **219** 88
[111] Bondzie V, Kleban P and Brown D A 1993 *J. Vac. Sci. Technol.* **11** 1946
[112] Heinze S, Schmatloch V and Kruse N 1995 *Surf. Sci.* **341** 124